Title

Histogram Analysis of Hepatobiliary Phase MR Imaging as a Quantitative Value for Liver Cirrhosis: Preliminary Observations

Journal

Yonsei Medical Journal, 55(3)

ISSN

0513-5796

Authors

Choi, Jin-Young
Kim, Honsoul
Sun, Mark
et al.

Publication Date

2014

DOI

10.3349/ymj.2014.55.3.651

Peer reviewed

Original Article

http://dx.doi.org/10.3349/ymj.2014.55.3.651
pISSN: 0513-5796, eISSN: 1976-2437

Yonsei Med J 55(3):651-659, 2014

YMJ

Histogram Analysis of Hepatobiliary Phase MR Imaging as a Quantitative Value for Liver Cirrhosis: Preliminary Observations

Jin-Young Choi,[1] Honsoul Kim,[1] Mark Sun,[2] and Claude B. Sirlin[2]

[1]Department of Radiology, Research Institute of Radiological Science, Yonsei University College of Medicine, Seoul, Korea;
[2]Department of Radiology, University of California, San Diego Medical Center, San Diego, CA, USA.

Received: June 12, 2013
Revised: August 21, 2013
Accepted: September 1, 2013
Corresponding author: Dr. Jin-Young Choi,
Department of Radiology,
Yonsei University College of Medicine,
50-1 Yonsei-ro, Seodaemun-gu,
Seoul 120-752, Korea.
Tel: 82-2-2228-7400, Fax: 82-2-393-3035
E-mail: gafield@yuhs.ac

· The authors have no financial conflicts of interest.

Purpose: To investigate whether histogram analysis of the hepatobiliary phase on gadoxetate enhanced-MRI could be used as a quantitative index for determination of liver cirrhosis. **Materials and Methods:** A total of 63 patients [26 in a normal liver function (NLF) group and 37 in a cirrhotic group] underwent gadoxetate-enhanced MRI, and hepatobiliary phase images were obtained at 20 minutes after contrast injection. The signal intensity of the hepatic parenchyma was measured at four different regions of interest (ROI) of the liver, avoiding vessels and bile ducts. Standard deviation (SD), coefficient of variation (CV), and corrected CV were calculated on the histograms at the ROIs. The distributions of CVs calculated from the ROI histogram were examined and statistical analysis was carried out. **Results:** The CV value was 0.041±0.009 (mean CV±SD) in the NLF group, while that of cirrhotic group was 0.071±0.020. There were statistically significant differences in the CVs and corrected CV values between the NLF and cirrhotic groups (p<0.001). The most accurate cut-off value among CVs for distinguishing normal from cirrhotic group was 0.052 (sensitivity 83.8% and specificity 88.5%). There was no statistically significant differences in SD between NLF and cirrhotic groups (p=0.307). **Conclusion:** The CV of histograms of the hepatobiliary phase on gadoxetate-enhanced MRI may be useful as a quantitative value for determining the presence of liver cirrhosis.

Key Words: Cirrhosis, gadoxetate disodium, magnetic resonance imaging, histogram

INTRODUCTION

The diagnosis of liver fibrosis and cirrhosis in patients with chronic liver disease is critical, as cirrhotic patients are at higher risk of developing end stage liver disease, portal hypertension, and hepatocellular carcinoma (HCC).[1,2] These sequelae are important causes of morbidity, mortality, and increasing health care costs.[3,4] The cumulative incidence of HCC is significantly higher in patients with severe fibrosis than in those with no or mild fibrosis.[5] Thus, the early detection and accurate staging of hepatic fibrosis or cirrhosis has become a critical issue in practice. Currently, liver biopsy is still the gold standard for the assessment of liver fibrosis. However, liver biopsy is invasive, difficult to repeat, and associated with significant patient morbidities. In

addition, liver biopsy is associated with interobserver variability and sampling errors.[6-8] The search for noninvasive imaging methods to assess liver fibrosis and cirrhosis has become an important endeavor. Although the presence of cirrhosis can be determined on the basis of liver contour abnormalities and portal hypertension stigmata using ultrasonography (US), computed tomography (CT), and conventional magnetic resonance (MR) imaging, these findings are insensitive in the detection of mild fibrosis and early cirrhosis.[9-11]

MR imaging has emerged as a promising modality for the assessment of diffuse liver disease. MR imaging provides excellent tissue contrast and high sensitivity to the effect of contrast agent,[12-14] allowing for visualization of hepatic texture that offers the potential of noninvasively diagnosing cirrhosis. Previous studies have reported that fibrosis grades can be accurately assessed using superparamagnetic iron oxides (SPIO) or double contrast material (SPIO plus gadolinium chelates) enhanced MR imaging.[15,16] Gadoxetate disodium is an MR imaging contrast agent that was developed for evaluating the hepatobiliary system.[17,18] After intravenous injection, gadoxetate disodium is gradually taken up by hepatocytes and is eventually excreted via the biliary system.[17] It is known that after gadoxetate is intravenously injected, it accumulates in hepatocytes and causes T1 shortening, which increases liver signal intensity (SI).[19] In patients with fibrosis, gadoxetate disodium accumulates and causes T1 shortening preferentially in the spared liver parenchyma, resulting in fibrotic bands appearing relatively hypointense.[20,21] For this reason, it may be possible to diagnose cirrhosis on gadoxetate-enhanced MR images on the basis of hepatic texture alterations.

A histogram is a useful tool in hepatic texture analysis (TA),[22,23] as it depicts the distribution of SI levels. We postulated that cirrhotic liver would show a wider range of SI values than normal liver on hepatobiliary phase MR imaging due to fibrotic bands. To our knowledge, there have not been studies exploring cirrhosis with histograms of hepatobiliary phase images using gadoxetate disodium-enhanced MR imaging. The purpose of this study was to investigate whether histogram analysis of hepatobiliary phase MR imaging could be used as a quantitative index for determination of liver cirrhosis.

Table 1. Causes of Liver Disease

Cause	No. of patients*
Hepatitis C virus	14 (37)
Hepatitis B virus	8 (22)
Alcohol intake	5 (14)
Nonalcoholic steatohepatitis	3 (8)
Autoimmune hepatitis	1 (3)
Recurrent pyogenic cholangitis	1 (3)
Hemochromatosis	1 (3)
Cryptogenic	4 (10)

*Numbers in parentheses are percentages.

MATERIALS AND METHODS

Patients

This retrospective study was compliant with the Health Insurance Portability and Accountability Act and was approved by our Institutional Review Board; the need for patient informed consent was waived. From April 2008 to February 2011, 285 patients who were suspected of having chronic liver disease or focal hepatic lesions clinically or at previously performed US or CT underwent gadoxetate (Eovist, Primovist; Bayer Healthcare Pharmaceuticals, Berlin, Germany) enhanced liver MRI. Among them, 128 patients were examined with a 3T MR scanner. We included the examinations with 3T MR scanners because 3T scanners have benefits in depicting fine details due to its high signal-to-noise ratio (SNR) than 1.5T scanners. Sixty-five patients were excluded for the following reasons: hepatectomy (n=11); poor biliary excretion (n=9); and metastatic disease (n=45). We excluded the patients with poor biliary excretion because adequate hepatobiliary phase images are not typically obtained in these patients.

Finally, a total of 63 patients (28 men, 35 women; age range, 21-90 years), including 37 patients with cirrhosis and 26 patients without liver disease, comprised the study cohort. Patients with suspected benign focal liver lesions in normal liver parenchyma were classified into a normal liver function (NLF) group (n=26). Patients with cirrhosis were classified into a cirrhotic group (n=37). The cirrhotic group (mean age, 56.7 years; range, 22-90 years) included 22 men (mean age, 59.7 years; range, 34-90 years) and 15 women (mean age, 52.4 years; range, 22-72 years), and the NLF group (mean age, 47.7 years; range, 21-73 years) included 6 men (mean age, 57.7 years; range, 36-73 years) and 20 women (mean age, 44.7 years; range, 21-63 years).

The most common etiologies of liver disease were hepatitis C, hepatitis B, and alcohol consumption (Table 1). The clinical diagnosis of liver cirrhosis was obtained by previous histologic examination or was clinically apparent (history, laboratory data, imaging study, etc). All NLF and cirrhotic

groups underwent standard clinical biochemical testing before the MR examination. Patients with cirrhosis (n=37) were classified into two groups according to Child-Pugh classification: a liver cirrhosis with Child-Pugh A group (n=33) and a liver cirrhosis with Child-Pugh B group (n=4). No patients showed liver cirrhosis with Child-Pugh C status. Laboratory data (bilirubin, albumin, and prothrombin time) for the NLF and cirrhotic groups are summarized in Table 2.

The NLF group comprised patients with suspected benign focal liver lesions (e.g., hemangioma or cyst) in normal liver parenchyma. Patients of the NLF group presented with hemangiomas (n=11), focal nodular hyperplasia (n=9), cholangitis (n=4), and cysts (n=2). Consecutive patients who met the following criteria were included as control subjects: gadoxetate-enhanced MR imaging performed during the study period for indications other than HCC surveillance or diffuse liver disease assessment; no documentation of active or past liver disease; no risk factors for liver disease (i.e., consumption of two or more alcoholic drinks daily, viral hepatitis, and/or drug abuse); NLF test results obtained within 3 months of the index MR examination; and negative viral serology test results (if available). Based on these criteria, we judged that focal lesions did not influence liver function in these cases.

MR imaging technique

MR imaging was performed using a 3T system (Signa Excite HD; GE Medical Systems, Milwaukee, WI, USA) with an eight-channel torso coil. The basic MR imaging protocol consisted of the following imaging sequences: breath hold two-dimensional dual echo axial T1-weighted sequence [in-phase and out-of-phase; repetition time msec/echo time msec, 150/4.2 (in phase) and 150/2.0 (out-of-phase)]; respiratory-triggered two-dimensional fat-suppressed axial T2-weighted fast spin-echo imaging [1200/72 (effective)]; and breath-hold gadoxetate disodium-enhanced hepatic arterial dominant, portal venous, and late dynamic phase imaging with a fat suppressed three-dimensional gradient echo sequence (3.0/1.4; field of view, 24-30×32-40 cm; image matrix, 320×224; flip angle, 15°; section thickness, 3.0-mm section thickness, with no gap; acquisition time, 90 sections per each phase during 11-second breath hold). Hepatobiliary phase imaging was performed with identical MR imaging parameters, except that the acquisition time was 90 sections during a 22-second breath hold, and the time was within 15-25 minutes (mean, 20.5 minutes) after an intravenous bolus injection of gadoxetate disodium, 0.025 mmol per kilogram of body weight.

Quantitative analysis

MR images were stored in digital imaging and communications in medicine (DICOM) format. Images were reviewed by one abdominal radiologist (J.Y.C.) concerning whether there are typical features of liver cirrhosis several morphologic changes including enlargement of the caudate lobe and the left lateral segment of the liver, atrophy of the right hepatic lobe and the left medial segment, nodularity of the liver surface, coarse liver architecture, ascites, splenomegaly, and the development of collaterals. The same radiologist selected circular, 2 cm^2 regions of interest (ROI), avoiding vessels and bile ducts. For each patient, images with circular ROIs were stored on a secondary console containing the Osirix DICOM viewer for Macintosh (Osirix, version 3.5.1; the Osirix Foundation, Geneva, Switzerland) (Fig. 1). Two ROIs were selected on each image from the right hepatic lobe and two ROIs from lateral/medial segments of the left hepatic lobe at the level of horizontal portion of right portal vein. If the ROIs were settled, the standard deviation (SD) and mean values within the ROIs were calculated automatically in the viewer. SNRs of the liver on hepatobiliary phase MRI scans were calculated as follows: liver SNR=liver SI/SD of background noise. The four ROIs were used to generate quantitative measurements of liver texture heterogeneity-specifically, SD and coefficient of variation (CV).

The CV of standard liver ROI was calculated as follows: $CV=SD_{liver}/SI_{liver}$, where SD_{liver} is the SD of the mean liver parenchyma SI and SI_{liver} is the mean SI of the liver parenchyma. Based on our observation that cirrhotic liver has a more heterogeneous texture (hypointense reticulations against a bright liver background) than does the homogeneous normal liver, the CV was used as a measure of regional liver texture heterogeneity. As image noise might contribute to variances in liver SI, we also calculated a corrected CV by subtracting the SD of the mean air SI from the SD of the mean liver parenchyma SI as follows: corrected $CV=(SD_{liver}$-

Table 2. Patient Characteristics

	NLF group (n=26)	Cirrhosis group (n=37)
Age	47.7	56.7
Total bilirubin (mg/dL)	0.56±0.3	1.0±0.7
Albumin (mg/dL)	4.37±0.3	4.0±0.6
Prothrombin time (sec)	12.2±1.0	12.9±1.5

NLF, normal liver function.
Values indicate mean±standard deviation.

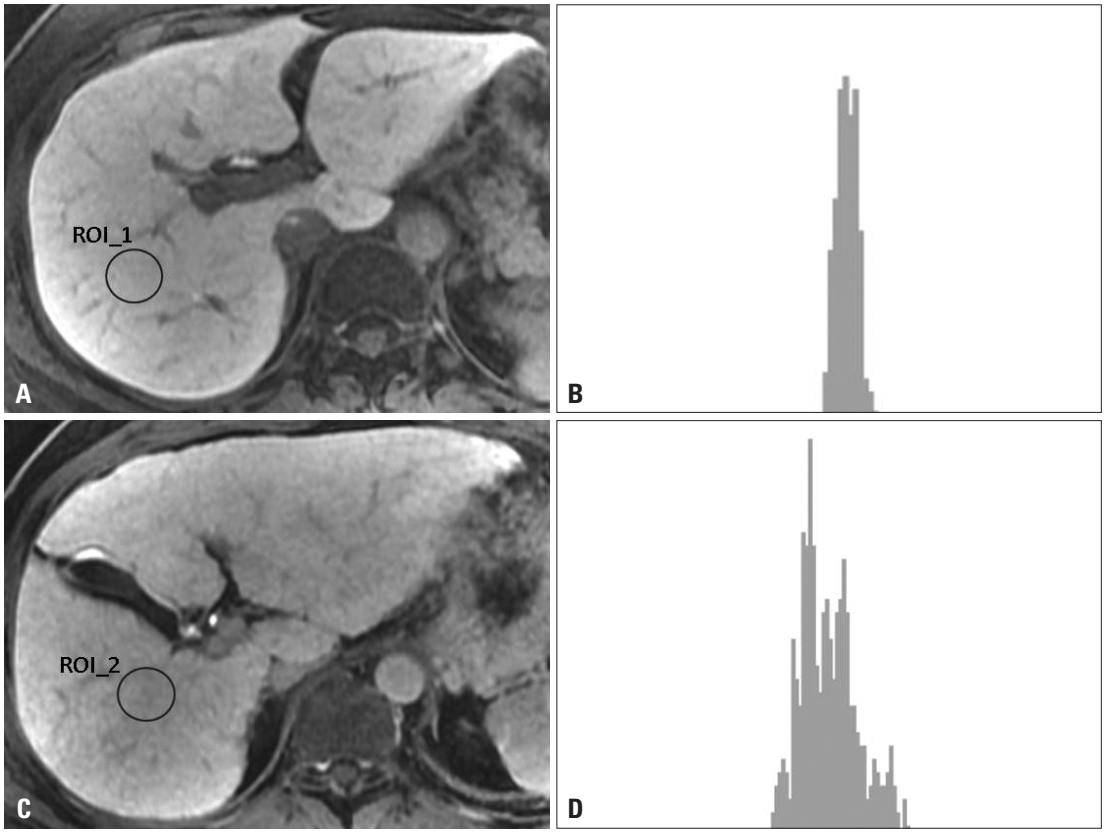

Fig. 1. Different histograms of normal function liver and cirrhotic liver on hepatobiliary phase images. (A) Axial T1-weighted hepatobiliary phase image obtained after injection of gadoxetate disodium in a 56-year-old woman with normal function liver and a coefficient of variation (CV) value of 0.035. (B) Histogram of selected region of interest (ROI) on hepatobiliary phase image shows a narrow distribution. The horizontal axis represents signal intensity of ROI and vertical axis shows frequency of observations. (C) Axial T1-weighted hepatobiliary phase image obtained after injection of gadoxetate disodium in a 48-year-old man with cirrhosis and a CV value of 0.062. (D) Histogram of selected ROI on hepatobiliary phase image shows a wide distribution.

SD_{air})/SI_{liver}.[15]

Statistical analysis

Data distributions were tested for normality with Shapiro-Wilk tests. A comparison of SI_{liver}, SD_{liver}, CVs, and corrected CVs of the groups was carried out using the unpaired Student's t-test. The Spearman's correlation test was used to assess the correlation of CV and corrected CV between NLF and cirrhotic groups. The optimal cut-off values of CVs for distinguishing normal and cirrhotic groups were calculated. The analysis was performed using SPSS software (17.0, SPSS Inc., Chicago, IL, USA). All p-values <0.05 were considered significant.

RESULTS

Of 37 cirrhotic patients, 35 patients showed definite morphological changes of cirrhosis on visual evaluation. The mean pixel size of the NLF group (0.64×0.42 mm) was comparable to the cirrhotic group (0.63×0.41 mm) (p>0.05). The mean SI±SD of the NLF group was 4146.7± 167.0 (maximum value 10715.3; minimum value 374.8), while that of the cirrhotic group was 1960.6±143.5 (maximum value 11065.9; minimum value 216.1). There were no statistically significant differences in liver SNR between the normal group and the cirrhotic group (mean SNR±SD; 37.10±12.7 for NLF group and 32.34±15.3 for cirrhosis group, p=0.184).

The mean SI, SD, CV, and corrected CV of the NLF and cirrhotic groups are shown in Fig. 2. The SD was 167.0± 142.1 (mean SD±SD) in the NLF group and 143.5±202.2 in the cirrhotic group. There was no statistically significant difference in SD between the NLF and cirrhotic groups (p= 0.307). In the NLF group, the CV value was 0.041±0.009 (mean CV±SD; maximum value 0.08; minimum value 0.03). In the cirrhotic group, the CV value was 0.071±0.020 (mean CV±SD; maximum value 0.17; minimum value 0.03). The CV values of the cirrhotic group were significantly higher than those of the NLF group (p<0.001). The CV for the NLF and cirrhotic groups showed a nonnormal

distribution (p<0.05, Shapiro-Wilk tests), showing skewness of 1.11 and 0.94, respectively (Fig. 3). The more skewed data for the NLF group than cirrhotic group might be explained by an inhomogeneous group of patients. The kurtosis of the NLF group was 2.03, while that of the cirrhotic group was 1.95. The Spearman's correlation test indicated that CV values were strongly correlated with the presence of cirrhosis with a value of 0.729 (p<0.001). The corrected CV values of the cirrhotic group were also higher than the NLF group (0.468±0.20 vs. 0.349±0.22) (p<0.001).

Sensitivities and specificities at various CV values were calculated for distinguishing normal from cirrhotic patients (Table 3). The cut-off value among CVs for distinguishing normal from cirrhotic patients with the best accuracy was 0.052 (sensitivity 83.8% and specificity 88.5%).

DISCUSSION

Our results suggest that histogram analysis of hepatobiliary phase MRI can be helpful for differentiating patients with NLF and those with cirrhosis. Among the parameters of histograms, CV and corrected CV values of histograms were significantly different between NLF and cirrhotic groups. Our study suggests that histogram analysis holds the potential to provide a quantitative index of liver cirrhosis. Cirrhosis induces several morphologic changes including enlargement of the caudate lobe and the left lateral segment of the liver, atrophy of the right hepatic lobe and the left medial segment, nodularity of the liver surface, coarse liver architecture, ascites, splenomegaly, and development of collaterals.[9,24-26] However, most are based on morphologic changes in the liver that occur late in progression of liver disease or secondary signs of portal hypertension. These findings have limited utility for the detection of early cirrhosis and the grading of advanced fibrosis. The diagnosis of hepatic fibrosis of an intermediate degree is difficult because hepatic parenchymal textural alterations are often subtle. Although there was overlap of CV values between the NLF and cirrhotic groups, we were able to reliably differentiate between the two groups with the CVs of hepatobiliary phase imaging. Our study also introduced a simple and practical method for determining the distribution of pixel values. With our method, the SD and average value of ROIs can be measured with the picture archiving and communication system (PACS) and the CV can be easily calculated. Accordingly, we suggest that CVs of the hepatobiliary phase

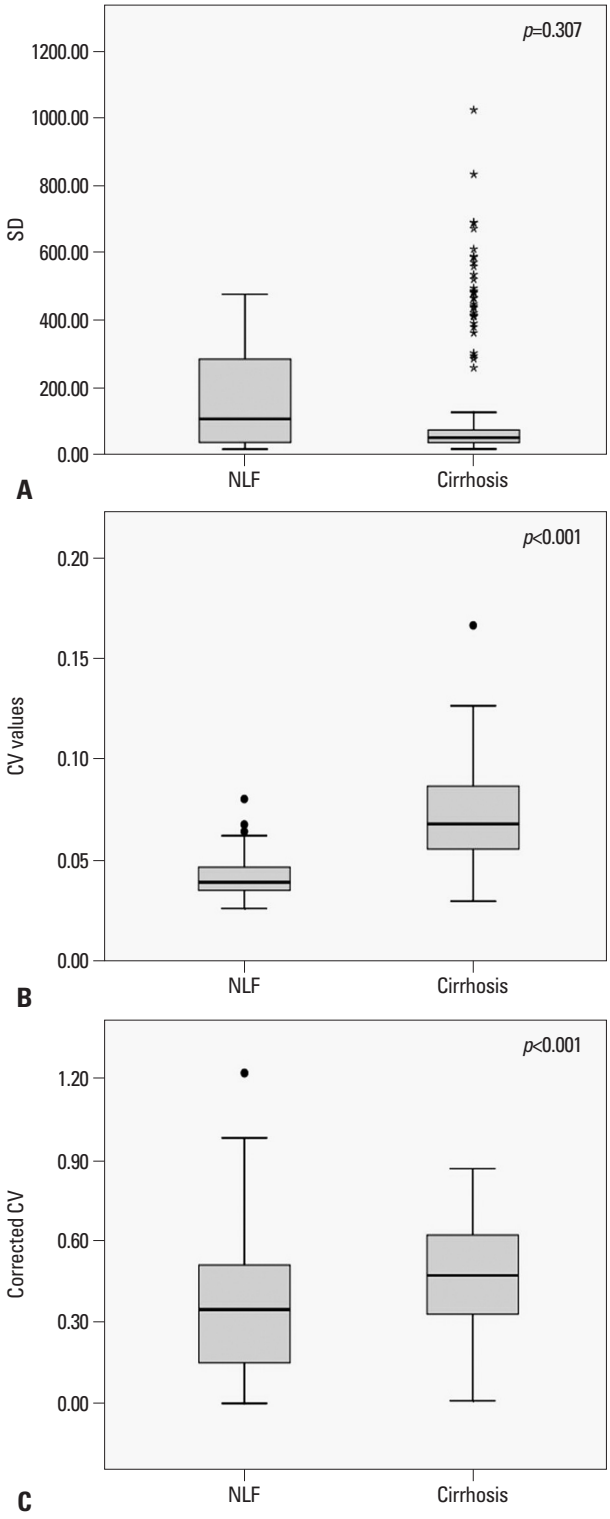

Fig. 2. Box plots show the results of analysis of (A) the SD, (B) CV values, and (C) corrected CV for the NLF and cirrhotic groups. Each box stretches from the 25th percentile at lower edge to the 75th percentile at upper edge; the median is shown as a line across the box. There are two adjacent values below and above the box: the largest value is below the upper inner limit and the smallest value is above the lower inner limit. Outside values below or above the inner limit but within the outer limit are outliers. Star marks in Fig. 2A indicates outlying values meaning wide range of pixel values in cirrhosis. SD, standard deviation; CV, coefficient of variation; NLF, normal liver function.

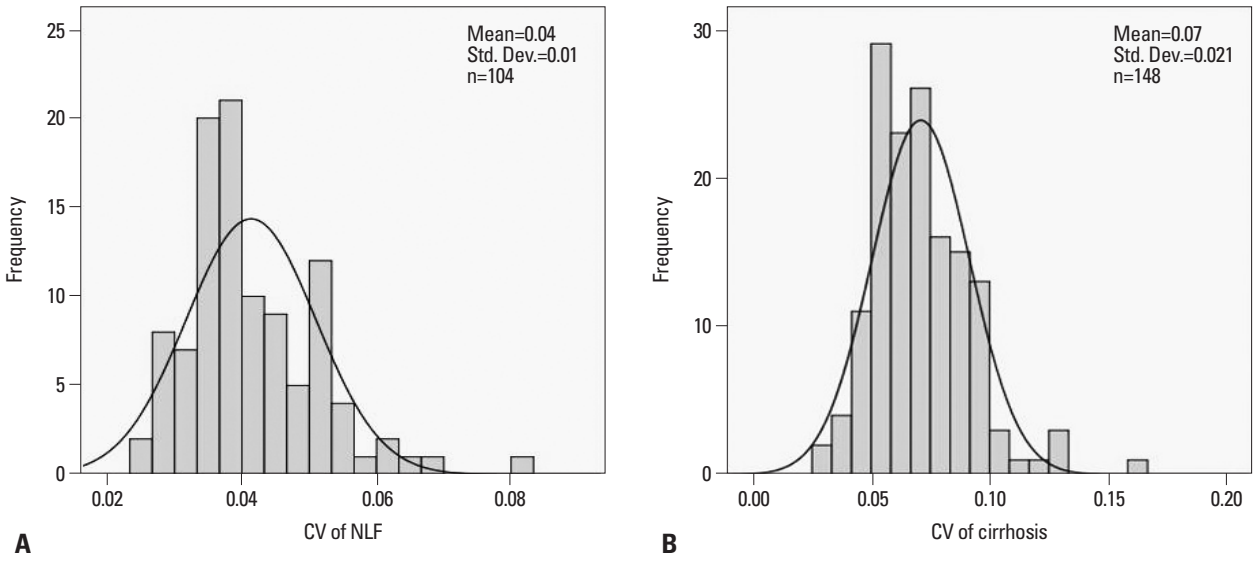

Fig. 3. Histograms of NLF and cirrhosis groups. (A) The CV for NLF group showed a normal distribution, showing a skewness value of 1.11. (B) The CV for cirrhosis group showed a normal distribution, showing a skewness value of 0.94. CV, coefficient of variation; NLF, normal liver function.

Table 3. Various Cut-Off Values of CV to Distinguish Normal Liver Function from Cirrhosis

Cut-off values	0.03	0.04	0.05	0.052	0.06	0.07	0.08
Sensitivity	99.3	98.0	88.5	83.8	68.9	44.6	27.0
Specificity	9.6	55.8	78.8	88.5	95.2	99.0	99.0

CV, coefficient of variation.
Values of sensitivity and specificity indicate percentage (%).

can be used as a screening measurement tool for evaluating hepatic parenchymal texture and aid in the diagnosis of cirrhosis in daily practice.

Biopsy remains the clinical reference standard for the diagnosis of liver fibrosis. Serum biomarkers for liver fibrosis have been described, but their clinical effectiveness has not been established. The development of noninvasive imaging methods to detect fibrosis has become a major interest for clinicians who hope for more efficient and effective serial follow-up of patients, documentation of temporal changes, and assessment of therapy response. Some investigators have proposed that it may be possible to diagnosis and grade fibrosis with MR imaging by measuring viscoelasticity[27-29] or water diffusion.[21,30] A different approach is to directly visualize fibrotic tissue. In previous reports, fibrosis has been depicted as hyperintense reticulations against a hypointense liver background after the administration of SPIOs or combination of SPIO and gadolinium-based contrast material.[15,16,31] The hyperintense reticulations, which are postulated to represent septal fibrosis, can be observed in cirrhotic liver tissue. Gadoxetate disodium-enhanced MR imaging has been suggested as a reliable method for staging hepatic fibrosis. Watanabe, et al.[21] reported that contrast enhancement index on gadoxetate disodium-enhanced MR imaging is more reliable for staging hepatic fibrosis than diffusion-weighted MR imaging and clinical parameters. Our results suggest that liver cirrhosis can be accurately evaluated using TA of the hepatobiliary phase. With a cut-off value of 0.052, sensitivity and specificity values greater than 84% were achieved. Combined texture and secondary imaging features would likely further improve diagnostic performance, although this was not evaluated in this study. Moreover, as contrast agent enhanced MRI is part of routine techniques for liver imaging, there is no need to acquire additional sequences such as diffusion-weighted sequence or MR elastography.

A histogram is a graphical representation of the distribution of data.[22,23] Histograms can be computed in the PACS program, which makes it possible to assess the distribution of each pixel value. In PACS, the SI value within a ROI is shown on the monitor by an automatic calculation of the selected ROI. The histogram illustrates how the pixels in an image are distributed by graphing the number of pixels, while the SD represents the variation in the SI values. The vertical axis shows the total number of pixels with a given value. The CV is a normalized measure of dispersion of a probability distribution that can be used when comparing between data sets with different units or widely different means. The CV values of the hepatobiliary phase on gadoxetate disodium-enhanced MRI that are calculated on the ROI histogram reflect the homogeneity or heterogeneity of the hepatic parenchyma. Smaller CV values are thought to represent normal liver, while larger CV values reflect the

possibility of cirrhotic liver in which with fibrotic bands are thought to cause reflections of various signal intensities. Although differences in the CV values between NLF and cirrhotic groups were observed, there was definite overlap of CV values between NLF and cirrhotic groups. This was presumably because variable stages of fibrosis were included in this study and small vessels or bile ducts could have been included in the ROIs. The evaluation of fibrosis, therefore, depends on the choice of ROI, which should be improved in the future.

Texture refers to the distribution of brightness and darkness within the image. TA is based on the quantification of complex mathematical patterns, which exist in the gray-level distribution of the pixels of images. TA evaluates the spatial location and SI of each pixel in the examined area.[32] There are many features that can be applied for TA. Among them, the statistical measurement methods represent the statistical aspect of texture evaluation, concerning the interrelationships among pixels. Other texture feature analysis approaches are based on models. Jirák, et al.[32] reported that the best discriminative feature for differentiating cirrhosis from normal was kurtosis; other differentiating features included difference entropy, gradient skewness, and skewness. Combination of texture parameters such as mean gray-scale value, contrast, angular second moment, or entropy have also been used for differentiating hepatic fibrosis from normal liver.[33] CV and corrected CV have been suggested as accurate quantitative scores for liver texture features.[15] Our TA is based only on the variability of SI on hepatobiliary phase images. More sophisticated texture features can be assessed and may facilitate better performance. Regarding the sequence of MR imaging, the equilibrium phase after administration of gadolinium-based contrast agent has been suggested to reflect the degree of fibrosis most accurately.[33] Compared to equilibrium phase of gadolinium-based contrast agent, hepatobiliary phase images using gadoxetate disodium have better contrast-to-noise ratio (CNR), resulting in superior conspicuity for fibrotic bands in cirrhotic liver. Therefore, hepatobiliary phase imaging may be the optimal sequence for evaluating TA.

Our study was limited by its retrospective design and inclusion of cirrhotic patients who had advanced fibrosis with obvious imaging stigmata of liver disease or based on clinical findings. Second, we could not analyze the data according to the grade of fibrosis because no histopathologic proof was obtained for cirrhotic patients. Further studies are needed to determine if this method can be used in grading hepatic fibrosis. Third, the enhancement of hepatobiliary phase depends on several factors although organic anionic transport polypeptides 8 (OATP8, also known as OATP1B1/3) are the dominant determinant.[34] OATP8 is thought to be responsible for uptake by hepatocytes of gadoxetic acid.[35] OATP8 represent members of the OATP superfamily that mediate the sodium-independent hepatic uptake of a diverse range of organic compounds including bile acids, thyroid hormones, bilirubin gluconides, steroid conjugates, and numerous drugs such as statins or sartans.[36] Therefore, hepatic uptake of gadoxetic acid may be influenced in patients taking these organic compounds because of competitive uptake. Also the SNR of the hepatobiliary phase may be influenced by modulating the flip angle. Increasing the flip angle in the hepatobiliary phase T1-weighted imaging increases the SNR of the liver, while decreasing the SNR of non-hepatocyte-containing tissues such as fibrosis results in an increased lesion to liver CNR with subsequent improved lesion conspicuity.[37] This effect is due to an increase in T1-weighting, resulting in an increase in contrast between hepatic fibrotic tissues and functioning hepatic parenchyma.[38,39] Thus the quantitative value in our study may not be applied equally when flip angle is modulated from its conventional setting (10-15°). Fourth, the pixel size of hepatobiliary phase was not exactly the same in each patient. However, the pixel size was comparable in both groups and there was no statistical difference therein between the two groups. Fifth, we did not evaluate the interobserver variability of the measurement of ROIs. This issue should be further studied in a larger series. Finally, we excluded patients with impaired hepatic enhancement because this group of patients cannot be effectively imaged with gadoxetate disodium-enhanced MRI. Considering that hepatic function is closely related to hepatic uptake of gadoxetate, this may have introduced a component of selection bias to our study.

In conclusion, the histogram analysis of hepatobiliary phase MRI reflects the homogeneity or heterogeneity of the hepatic parenchyma. The CV values of histogram on hepatobiliary phase can be used as a quantitative value that can determine the presence of liver cirrhosis.

ACKNOWLEDGEMENTS

This study was supported by a faculty research grant of Yonsei University College of Medicine (4-2011-0897).

REFERENCES

1. Afdhal NH, Nunes D. Evaluation of liver fibrosis: a concise review. Am J Gastroenterol 2004;99:1160-74.
2. Schuppan D, Afdhal NH. Liver cirrhosis. Lancet 2008;371:838-51.
3. Buti M, San Miguel R, Brosa M, Cabasés JM, Medina M, Angel Casado M, et al. Estimating the impact of hepatitis C virus therapy on future liver-related morbidity, mortality and costs related to chronic hepatitis C. J Hepatol 2005;42:639-45.
4. Talwalkar JA. Economic impact of hospitalization for end-stage liver disease. Am J Gastroenterol 2002;97:1562.
5. Tokita H, Fukui H, Tanaka A, Kamitsukasa H, Yagura M, Harada H, et al. Risk factors for the development of hepatocellular carcinoma among patients with chronic hepatitis C who achieved a sustained virological response to interferon therapy. J Gastroenterol Hepatol 2005;20:752-8.
6. Froehlich F, Lamy O, Fried M, Gonvers JJ. Practice and complications of liver biopsy. Results of a nationwide survey in Switzerland. Dig Dis Sci 1993;38:1480-4.
7. Perrault J, McGill DB, Ott BJ, Taylor WF. Liver biopsy: complications in 1000 inpatients and outpatients. Gastroenterology 1978;74:103-6.
8. Terjung B, Lemnitzer I, Dumoulin FL, Effenberger W, Brackmann HH, Sauerbruch T, et al. Bleeding complications after percutaneous liver biopsy. An analysis of risk factors. Digestion 2003;67:138-45.
9. Ito K, Mitchell DG. Imaging diagnosis of cirrhosis and chronic hepatitis. Intervirology 2004;47:134-43.
10. Schwenzer NF, Springer F, Schraml C, Stefan N, Machann J, Schick F. Non-invasive assessment and quantification of liver steatosis by ultrasound, computed tomography and magnetic resonance. J Hepatol 2009;51:433-45.
11. Vitellas KM, Tzalonikou MT, Bennett WF, Vaswani KK, Bova JG. Cirrhosis: spectrum of findings on unenhanced and dynamic gadolinium-enhanced MR imaging. Abdom Imaging 2001;26:601-15.
12. Hammerstingl R, Zangos S, Schwarz W, Rosen T, Bechstein WO, Balzer T, et al. Contrast-enhanced MRI of focal liver tumors using a hepatobiliary MR contrast agent: detection and differential diagnosis using Gd-EOB-DTPA-enhanced versus Gd-DTPA-enhanced MRI in the same patient. Acad Radiol 2002;9 Suppl 1:S119-20.
13. Talwalkar JA, Yin M, Fidler JL, Sanderson SO, Kamath PS, Ehman RL. Magnetic resonance imaging of hepatic fibrosis: emerging clinical applications. Hepatology 2008;47:332-42.
14. Bluemke DA, Sahani D, Amendola M, Balzer T, Breuer J, Brown JJ, et al. Efficacy and safety of MR imaging with liver-specific contrast agent: U.S. multicenter phase III study. Radiology 2005;237:89-98.
15. Aguirre DA, Behling CA, Alpert E, Hassanein TI, Sirlin CB. Liver fibrosis: noninvasive diagnosis with double contrast material-enhanced MR imaging. Radiology 2006;239:425-37.
16. Lucidarme O, Baleston F, Cadi M, Bellin MF, Charlotte F, Ratziu V, et al. Non-invasive detection of liver fibrosis: is superparamagnetic iron oxide particle-enhanced MR imaging a contributive technique? Eur Radiol 2003;13:467-74.
17. Hamm B, Staks T, Mühler A, Bollow M, Taupitz M, Frenzel T, et al. Phase I clinical evaluation of Gd-EOB-DTPA as a hepatobiliary MR contrast agent: safety, pharmacokinetics, and MR imaging. Radiology 1995;195:785-92.
18. Reimer P, Rummeny EJ, Shamsi K, Balzer T, Daldrup HE, Tombach B, et al. Phase II clinical evaluation of Gd-EOB-DTPA: dose, safety aspects, and pulse sequence. Radiology 1996;199:177-83.
19. Ni Y, Marchal G, Lukito G, Yu J, Mühler A, Baert AL. MR imaging evaluation of liver enhancement by Gd-EOB-DTPA in selective and total bile duct obstruction in rats: correlation with serologic, microcholangiographic, and histologic findings. Radiology 1994;190:753-8.
20. Tsuda N, Okada M, Murakami T. New proposal for the staging of nonalcoholic steatohepatitis: evaluation of liver fibrosis on Gd-EOB-DTPA-enhanced MRI. Eur J Radiol 2010;73:137-42.
21. Watanabe H, Kanematsu M, Goshima S, Kondo H, Onozuka M, Moriyama N, et al. Staging hepatic fibrosis: comparison of gadoxetate disodium-enhanced and diffusion-weighted MR imaging--preliminary observations. Radiology 2011;259:142-50.
22. Săftoiu A, Gheonea DI, Ciurea T. Hue histogram analysis of real-time elastography images for noninvasive assessment of liver fibrosis. AJR Am J Roentgenol 2007;189:W232-3.
23. Maeda K, Utsu M, Kihaile PE. Quantification of sonographic echogenicity with grey-level histogram width: a clinical tissue characterization. Ultrasound Med Biol 1998;24:225-34.
24. Aubé C, Oberti F, Korali N, Namour MA, Loisel D, Tanguy JY, et al. Ultrasonographic diagnosis of hepatic fibrosis or cirrhosis. J Hepatol 1999;30:472-8.
25. Brancatelli G, Federle MP, Ambrosini R, Lagalla R, Carriero A, Midiri M, et al. Cirrhosis: CT and MR imaging evaluation. Eur J Radiol 2007;61:57-69.
26. Ito K, Mitchell DG, Siegelman ES. Cirrhosis: MR imaging features. Magn Reson Imaging Clin N Am 2002;10:75-92.
27. Yin M, Talwalkar JA, Glaser KJ, Manduca A, Grimm RC, Rossman PJ, et al. Assessment of hepatic fibrosis with magnetic resonance elastography. Clin Gastroenterol Hepatol 2007;5:1207-13.
28. Asbach P, Klatt D, Hamhaber U, Braun J, Somasundaram R, Hamm B, et al. Assessment of liver viscoelasticity using multifrequency MR elastography. Magn Reson Med 2008;60:373-9.
29. Huwart L, Sempoux C, Salameh N, Jamart J, Annet L, Sinkus R, et al. Liver fibrosis: noninvasive assessment with MR elastography versus aspartate aminotransferase-to-platelet ratio index. Radiology 2007;245:458-66.
30. Annet L, Peeters F, Abarca-Quinones J, Leclercq I, Moulin P, Van Beers BE. Assessment of diffusion-weighted MR imaging in liver fibrosis. J Magn Reson Imaging 2007;25:122-8.
31. Faria SC, Ganesan K, Mwangi I, Shiehmorteza M, Viamonte B, Mazhar S, et al. MR imaging of liver fibrosis: current state of the art. Radiographics 2009;29:1615-35.
32. Jirák D, Dezortová M, Taimr P, Hájek M. Texture analysis of human liver. J Magn Reson Imaging 2002;15:68-74.
33. Kato H, Kanematsu M, Zhang X, Saio M, Kondo H, Goshima S, et al. Computer-aided diagnosis of hepatic fibrosis: preliminary evaluation of MRI texture analysis using the finite difference method and an artificial neural network. AJR Am J Roentgenol 2007;189:117-22.
34. Kitao A, Matsui O, Yoneda N, Kozaka K, Shinmura R, Koda W, et al. The uptake transporter OATP8 expression decreases during multistep hepatocarcinogenesis: correlation with gadoxetic acid enhanced MR imaging. Eur Radiol 2011;21:2056-66.
35. Tsuboyama T, Onishi H, Kim T, Akita H, Hori M, Tatsumi M, et al. Hepatocellular carcinoma: hepatocyte-selective enhancement at gadoxetic acid-enhanced MR imaging--correlation with expres-

sion of sinusoidal and canalicular transporters and bile accumulation. Radiology 2010;255:824-33.
36. Nassif A, Jia J, Keiser M, Oswald S, Modess C, Nagel S, et al. Visualization of hepatic uptake transporter function in healthy subjects by using gadoxetic acid-enhanced MR imaging. Radiology 2012;264:741-50.
37. Bashir MR, Husarik DB, Ziemlewicz TJ, Gupta RT, Boll DT, Merkle EM. Liver MRI in the hepatocyte phase with gadolinium-EOB-DTPA: does increasing the flip angle improve conspicuity and detection rate of hypointense lesions? J Magn Reson Imaging 2012;35:611-6.
38. Stelter L, Grieser C, Fernándes CM, Rothe JH, Streitparth F, Seehofer D, et al. Flip angle modulations in late phase Gd-EOB-DTPA MRI improve the identification of the biliary system. Eur J Radiol 2012;81:e991-5.
39. Bashir MR, Merkle EM. Improved liver lesion conspicuity by increasing the flip angle during hepatocyte phase MR imaging. Eur Radiol 2011;21:291-4.